Neuron, Vol. 48, 859–872, December 8, 2005, Copyright ©2005 by Elsevier Inc. DOI 10.1016/j.neuron.2005.10.032

Negative BOLD Differentiates Visual Imagery and Perception

Amir Amedi,[1,*] Rafael Malach,[2] and Alvaro Pascual-Leone[1,*]
[1] Center for Noninvasive Brain Stimulation
Department of Neurology
Beth Israel Deaconess Medical Center
Harvard Medical School
Boston, Massachusetts 02115
[2] Department of Neurobiology
Weizmann Institute of Science
Rehovot 76100
Israel

Summary

Recent studies emphasize the overlap between the neural substrates of visual perception and visual imagery. However, the subjective experiences of imagining and seeing are clearly different. Here we demonstrate that *deactivation* of auditory cortex (and to some extent of somatosensory and subcortical visual structures) as measured by BOLD functional magnetic resonance imaging unequivocally differentiates visual imagery from visual perception. During visual imagery, auditory cortex deactivation negatively correlates with activation in visual cortex and with the score in the subjective vividness of visual imagery questionnaire (VVIQ). Perception of the world requires the merging of multisensory information so that, during seeing, information from other sensory systems modifies visual cortical activity and shapes experience. We suggest that pure visual imagery corresponds to the isolated activation of visual cortical areas with concurrent deactivation of "irrelevant" sensory processing that could disrupt the image created by our "mind's eye."

Introduction

Seeing an object is clearly a different experience from imagining it. In fact, when experiential boundaries between perceiving and imagining blur, we speak of psychosis and hallucinations. Nevertheless, recent studies emphasize the overlap in the neural substrates supporting visual perception and visual imagery (Ishai and Sagi, 1995; Ishai et al., 2000; Kosslyn et al., 1999; Kreiman et al., 2000; Lambert et al., 2004; Mechelli et al., 2004; O'Craven and Kanwisher, 2000). For instance, most of the neurons in medial temporal cortex fire not only during both visual perception and imagery, but also share identical stimulus selectivity (Kreiman et al., 2000). One can predict whether an imagined object during an fMRI scan was a face or a house based on the magnitude of activity in the areas that are differentially activated during the perception of faces or objects (O'Craven and Kanwisher, 2000). Furthermore, it has been shown that visual imagery activates visual cortex in a retinotopic manner (Klein et al., 2004). So, if the activated brain areas are so similar, why is our experience so different? We raise here the possibility that fundamental differences in brain activity between imagery and perception might exist.

We argue that visual perception is inextricably associated with a multisensory experience of the object (Amedi et al., 2005; Beauchamp, 2005; Driver and Spence, 1998; Pascual-Leone et al., 2005; Pascual-Leone and Hamilton, 2001; Stein and Meredith, 1993). A number of recent findings are consistent with this notion. For example, early visual cortical areas are engaged in the processing of nonvisual information (Merabet et al., 2004), and the lateral occipital complex is engaged in shape discrimination of objects, regardless of the sensory modality that the information is presented in (Amedi et al., 2001; Beauchamp, 2005; Zhang et al., 2004). However, we hypothesize that imagery can be multisensory or purely visual. Often, imagery involves evoking the visual image of an object or behavior, along with its sounds, tactile impressions, proprioceptive input, and associated motor actions. Such a form of mental imagery can shape motor cortical outputs (Pascual-Leone et al., 1995). In contrast, under appropriate instruction, imagery can be purely visual, simply involving seeing "with the mind's eye" a given object or pattern and over-riding conflicting sensory stimulation coming from other modalities. In such instances, the activation of visual areas is critical (Kosslyn et al., 1999). Given this hypothesized contrast between "multisensory visual perception" and "purely visual mental imagery," we studied the difference between visual perception and visual imagery of objects in brain activity as indexed by negative and positive BOLD signal measured with functional magnetic resonance imaging (fMRI).

Until recently, most studies focused on reporting only an elevation in the fMRI BOLD signal, namely the positive BOLD. The fMRI positive BOLD signal is a physiologic process associated with a corresponding change in blood flow, blood oxygenation metabolism, local field potentials, and neural activity (for review see Logothetis and Wandell, 2004). Growing evidence suggests that, similarly, negative BOLD signal is a physiologic process that is correlated with a corresponding decrease in cerebral blood flow, oxygen consumption (Shmuel et al., 2002), and neuronal activity (A. Shmuel et al., 2003, NeuroImage, abstract), as opposed to an artifact due to image analysis or the shunting of blood flow (Laurienti, 2004; Shmuel et al., 2002; Wade, 2002). Thus, negative BOLD signal indicates *less* neural processing for a given task as compared to a given baseline (Laurienti, 2004; Shmuel et al., 2002; Wade, 2002; A. Shmuel et al., 2003, NeuroImage, abstract). Most studies on negative BOLD signal have focused on a network of posterior-medial, posterior-lateral, and ventro-medial prefrontal cortex originally referred to as the "default brain" network (Greicius and Menon, 2004; Raichle et al., 2001). This network is deactivated by a variety of goal-directed cognitive functions in various sensory modalities (Gusnard and Raichle, 2001; Greicius and Menon, 2004).

*Correspondence: aamedi@bidmc.harvard.edu (A.A.); apleone@bidmc.harvard.edu (A.P.-L.)

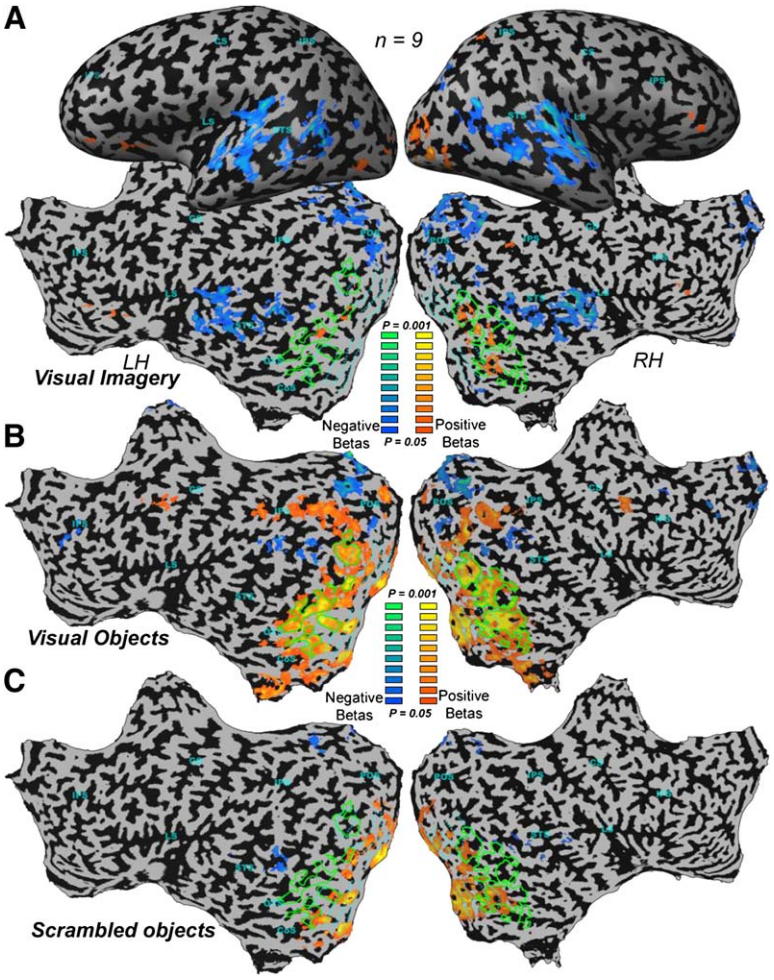

Figure 1. Statistical Parametric Maps of Positive and Negative BOLD Visual Imagery and Perception

Statistical parametric maps showing significant activation (red to yellow scale) and significant deactivation (blue to green scale) in a group of nine subjects, for visual imagery of objects (VI; [A]) versus a rest baseline condition, for visual object recognition (VO; [B]), and for viewing highly scrambled versions of the same objects (SCR; [C]). Group results are presented on a full Talairach-normalized brain of both cortical hemispheres. The most interesting result is the specific deactivation of auditory cortex to VI, but not to VO and SCR. This is in addition to positive activations in typical visual and prefrontal areas and deactivation for both VI and VO in typical "default" brain areas. The cyan dotted lines represent the borders of retinotopic areas (area V1–V4v in the ventral stream and V1–V7 in the dorsal stream). The green line represents object-related areas defined by the VO versus SCR contrasts. LS, lateral sulcus; STS, superior temporal sulcus; POS, parietal occipital sulcus; CS, cental sulcus; IFS, Inferior frontal sulcus; OTS, occipital temporal sulcus; CoS, collateral sulcus.

Other studies have investigated negative BOLD signal in sensory areas during simple perceptual tasks (Laurienti et al., 2002). Here we investigate the brain's deactivation pattern during visual imagery and compare it to the neural correlates of visual perception. We also correlate the magnitude of the activation or deactivation in different regions of interest (ROIs) and across the entire brain to the subjective report of the vividness of visual imagery questionnaire (VVIQ). Finally, we investigate the specific structures in the brain that correlate with the exact time course of seeds in visual and auditory cortices (frequently referred to as assessing "functional connectivity") during visual imagery and perception.

Results

Negative and Positive BOLD during Visual Imagery and Visual Perception

We measured brain activity, as indexed by fMRI BOLD signal, while sighted participants either performed a visual objects recognition task (VO), viewed scrambled images of the same objects (SCR), or created vivid mental images of familiar objects retrieved from memory (VI). As contrasted with rest, both VO and SCR tasks show positive BOLD activation in specific visual brain regions and show negative BOLD activation in medial posterior and lateral posterior areas (e.g., Raichle et al., 2001) (Figures 1B and 1C, respectively). During VI (Figure 1A), positive activation involves visual object areas (e.g., lateral occipital complex [LOC]) and retinotopic areas, as well as prefrontal and parietal areas, in concordance with previous reports (Ishai and Sagi, 1995; Ishai et al., 2000; Kosslyn et al., 1999; Kreiman et al., 2000; Lambert et al., 2004; Mechelli et al., 2004; O'Craven and Kanwisher, 2000).

The posterior cingulate/medial parietal area (PC), a central component of the "default brain" areas (Raichle et al., 2001), shows robust and similar deactivations during both VO and VI (Figure 2). The stronger deactivation during VO in comparison to SCR (where subjects were requested only to passively fixate) is consistent with the view that default brain areas are deactivated during "goal-directed actions" (Greicius and Menon, 2004; Raichle et al., 2001). This study shows that VI also deactivates this network and that the magnitude of this deactivation is similar to that found during VO (paired t test $p > 0.9$).

The main finding is that during VI we observed negative activation in bilateral auditory areas (Figure 1A), including planum temporale and Heschl's gyrus (HG, location of primary auditory cortex A1) and several other specific cortical and subcortical areas (not shown on cortex reconstruction, Figure 3). In contrast, the deactivation pattern associated with visual perception is

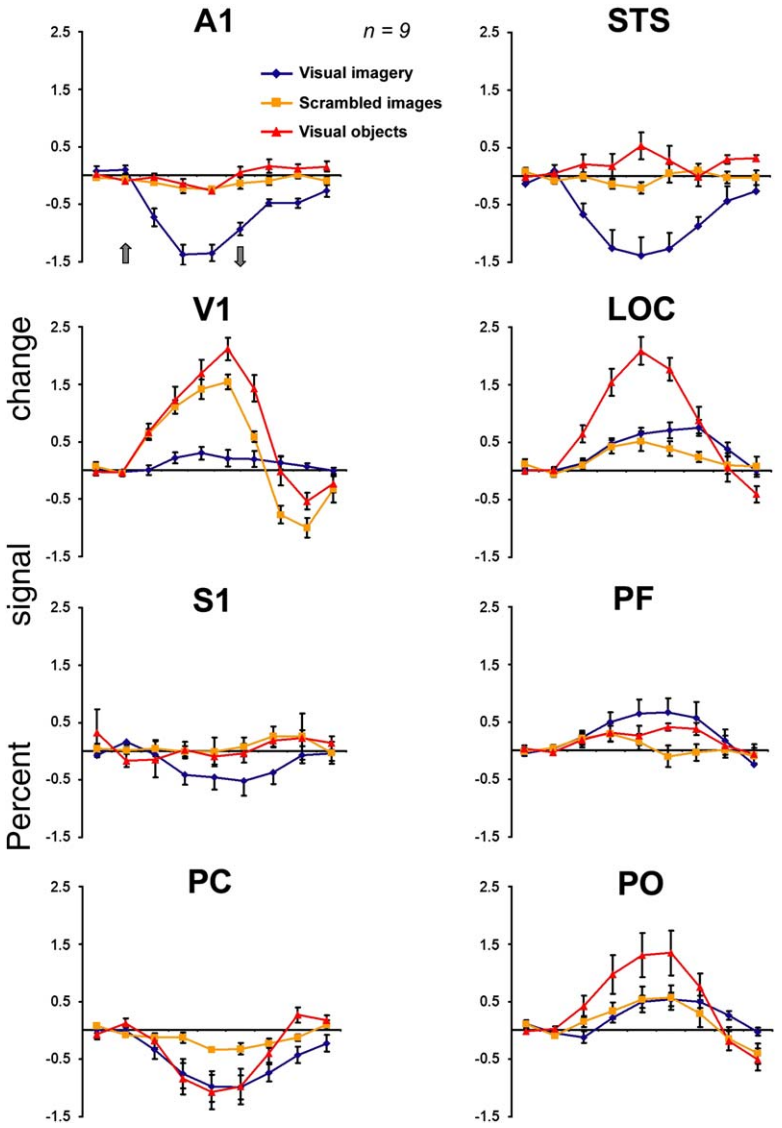

Figure 2. Average Time Course of Activation in Different Regions of Interest

The average time courses of activation for the three experimental conditions (VI, blue diamonds; VO, red triangles; SCR, orange squares; average percent signal changes across subjects ± SEM) are presented in eight regions of interest (ROIs). These are primary auditory cortex (A1); superior temporal sulcus (STS); primary visual cortex (V1); the lateral-occipital-complex (LOC); post-central gyrus (PCG/S1); inferior prefrontal cortex (PF); posterior cingulate "default brain" area (PC); and occipito-parietal cortex (PO ROI). (For details on ROI selection criteria see Experimental Procedures). Auditory ROIs (A1 and STS) show robust deactivation for VI with typical hemodynamic response patterns while showing negligible response to VO. In contrast, in visual areas (V1, LOC, and PO) there is robust activation for visual perception and positive, weaker activation for visual imagery, in agreement with the reported overlap for imagery and perception in the relevant sensory areas. S1 shows a similar pattern of deactivation for visual imagery as in early auditory cortex (though smaller in magnitude) and a negligible response to visual VO and SCR conditions. The PF ROI shows significant activation for visual imagery, in agreement with the top-down hypothesis for VI. Interestingly, posterior to the parieto-occipital sulcus (PO), there is a positive activation for both VO and VI, while anterior to this sulcus, the PC default brain area shows a robust and similar deactivation for both the VO and VI tasks. Thus, it seems that the parieto-occipital sulcus can serve as an anatomical marker separating activation and deactivation for both VO and VI.

almost entirely limited to the default brain network, with very few significant voxels in auditory cortex (Figures 1B and 1C for VO and SCR, respectively). This finding is also reflected in the time course of the fMRI hemodynamic response in the relevant regions of interest (ROIs) pooled over all subjects in auditory, visual, somatosensory, and prefrontal cortices (Figure 2). HG shows robust deactivation during VI with a typical hemodynamic response (average percent signal change ± SD = −1.1 ± 0.24). In contrast, a much weaker and nonsignificant deactivation was found during SCR (−0.15 ± 0.11), and no deactivation was found during VO (−0.06 ± 0.14). This demonstrates that the deactivation of auditory cortex is relatively specific for VI. Indeed, we found significantly more deactivation in A1 during imagery than during perception of objects (VI versus VO; $p < 0.005$; paired t test, Bonferroni corrected for multiple comparisons).

Deactivation during VI is not limited to early auditory areas. The superior temporal sulcus ROI (STS) also reveals robust negative BOLD to VI with some *positive* BOLD during VO (see Beauchamp et al., 2004). This results in a highly significant difference in the percent signal change between the two conditions (paired t test, $p < 0.001$ corrected). A similar pattern of deactivation (though smaller in magnitude and variable in laterality across subjects) is also evident in the post-central gyrus, with similar differences between VO and VI (paired t test, $p < 0.05$ corrected).

In contrast, visual areas that are strongly activated during VO also show activation, though significantly weaker, during VI (Figure 2; paired t test, $p < 0.005$ corrected for both V1 and LOC). This is compatible with previous studies of visual imagery (Ishai et al., 2000, 2002; O'Craven and Kanwisher, 2000). There is also activation during VI in prefrontal cortex (PF; Figure 2), which might be attributed to the hypothesized top-down role of PF cortex in the initiation of the imagery process (Ishai et al., 2000, 2002; Mechelli et al., 2004). Interestingly, the absolute magnitude of deactivation in auditory cortex during VI is larger than that of positive activation in visual cortex in the same condition and is comparable to the activation in visual cortex during VO or SCR (Figure 2) or of auditory cortex during perception of pure tones (data not shown).

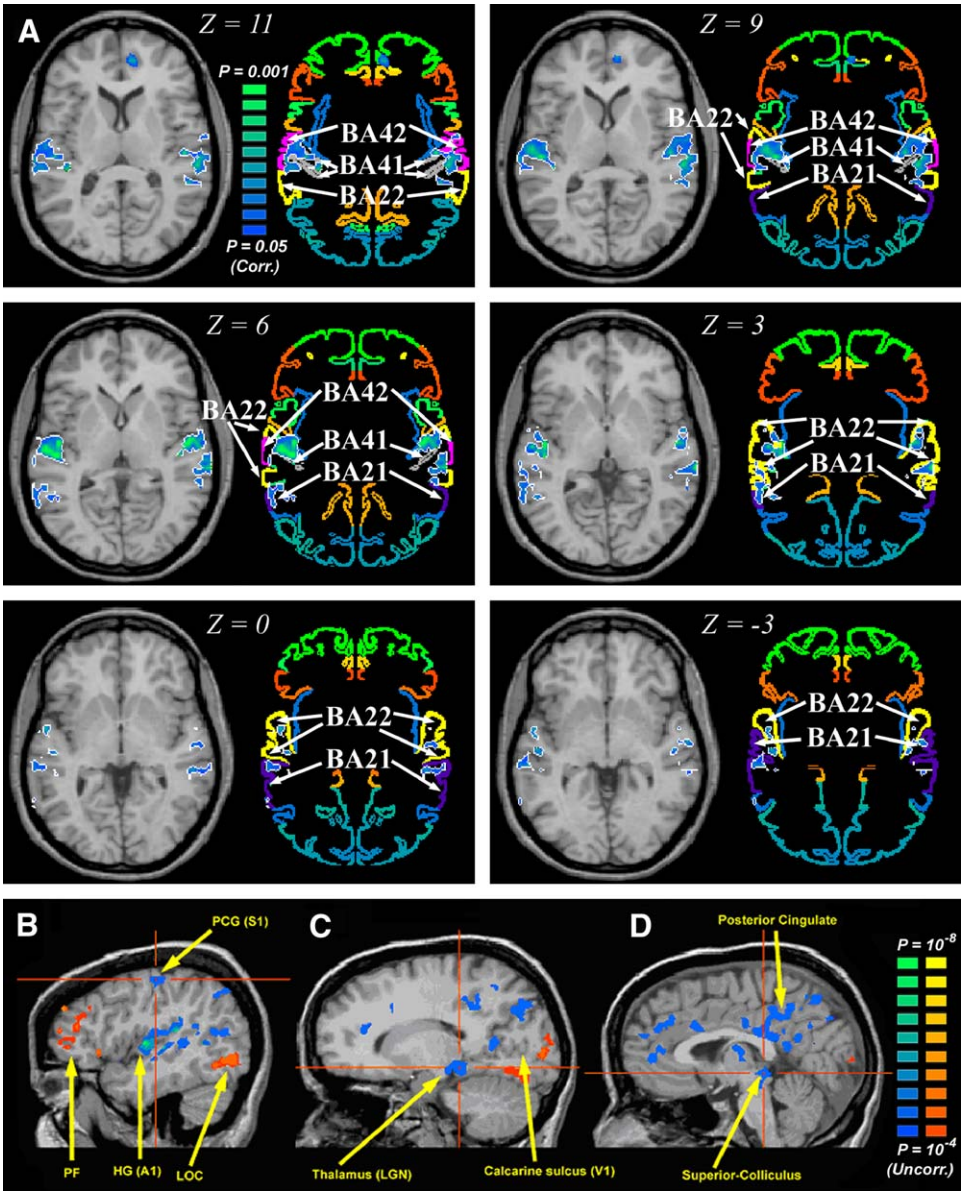

Figure 3. Statistical Parametric Maps of VI Activation and Deactivation Presented on Slices of Cortical and Subcortical Areas and on Corresponding Axial Slices Depicting Brodmann Areas

(A) Deactivation for VI in auditory cortex presented on axial anatomical slices in Talairach space (left). The same statistical parametric maps were projected onto corresponding axial slices depicting Brodmann areas (right). Deactivation was located in primary auditory cortex (BA41) and associative auditory cortex, located in superior temporal gyrus (BA42 and BA22). Some activation can also be seen in BA21 but to a lesser extent. (B) Deactivation for VI is evident also in somatosensory cortex and subcortical visual areas. The figure presents the activation pattern for visual imagery versus rest using a less conservative significance threshold ($p < 0.0001$ uncorrected for multiple comparisons in (B)–(D) for both positive and negative activations; scales hot and cold colors, respectively). Activation can be seen in the post-central gyrus bilaterally (PCG, where primary somatosensory cortex is located). (C) The thalamus, including parts of the lateral geniculate nucleus (LGN) and (D) the superior colliculus. These findings suggests that deactivation during visual imagery is evident also in bottom-up visual input pathways and other sensory modalities. However, these results should be taken tentatively, due to the less conservative threshold level used.

In order to identify further the localization of the deactivation pattern during VI, we projected the activations on axial slices and onto a corresponding Talairach normalized brain of Brodmann areas (Figure 3). Deactivation is evident in all subdivisions of auditory cortex, including primary auditory cortex (BA41), associative auditory cortex located primarily in superior temporal gyrus (BA42 and BA22), and stretching toward BA21. Lowering the threshold to $p < 0.0001$ uncorrected, clusters are found in the lateral geniculate nucleus (LGN; Figure 3C) and superior colliculus (SC; Figure 3D), as well as in the postcentral gyrus bilaterally (Figure 3B).

Single-subject statistical parametric maps show that deactivation of auditory cortex during VI is a highly consistent phenomenon present in both hemispheres of all subjects studied (Figure 4). As illustrated by Figure 4, deactivation in all subjects involves early auditory cortex in superior temporal gyrus. To further test the relations

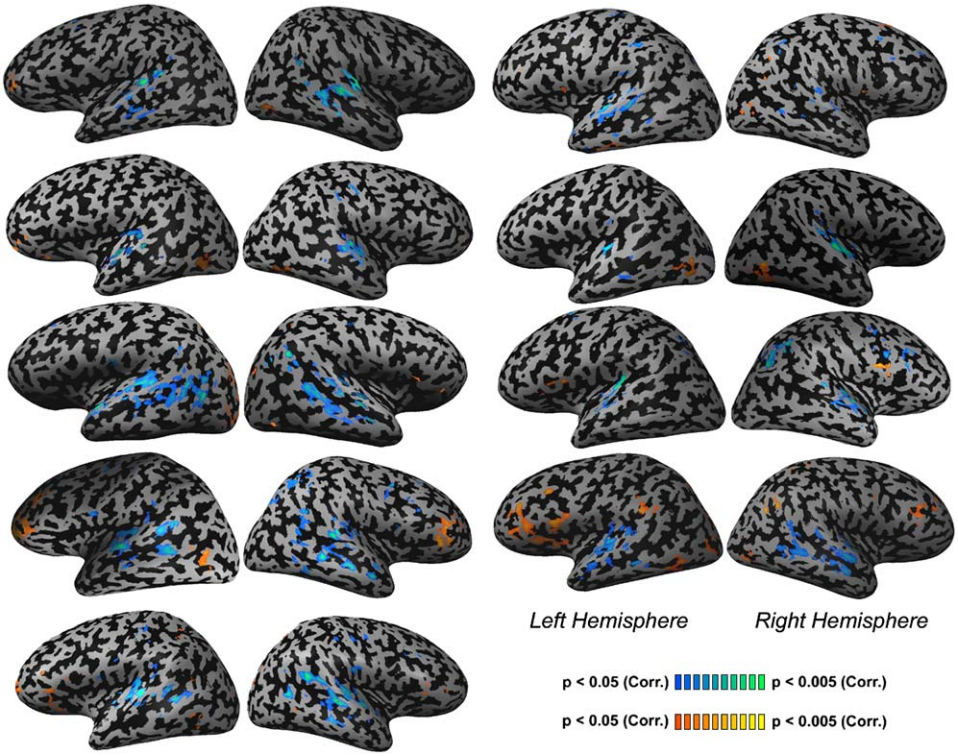

Figure 4. Visual Imagery Results in Significant Deactivation in Auditory Cortex of All Individual Subjects

The visual imagery versus rest contrast is presented ($p < 0.05$ corrected for multiple comparisons) on the individual inflated brain reconstruction of all nine subjects. Positive and negative BOLD are depicted by orange-to-red colors and blue-to-green colors, respectively.

between early auditory cortex and deactivation during VI, we conducted an external pure tones localizer to identify the voxels within HG showing significant response to pure tones (Figure 5A). Then we examined the activation profile of these voxels to the VI, VO, and SCR experimental conditions, finding robust deactivation to VI and negligible response to VO or SCR (Figure 5B). The VI deactivation follows a typical hemodynamic response function (opposite in polarity to the typical positive hemodynamic response). Furthermore, when we analyzed for each subject the response to VI of each individual voxel within HG showing significant response to pure tones, we found that in all cases the vast majority of voxels showed deactivation during VI (Figure 5B).

Finally, to test the differences in the deactivation level between VI and VO across the entire brain, we used a group-level random-effect analysis approach (Figure 6). We performed a conjunction analysis of VI versus VO with voxels showing deactivation to VI versus baseline (i.e., voxels having negative parameter estimators to VI in the general-linear model). The vast majority of these voxels are located in the auditory cortex bilaterally, including early auditory cortex in the superior temporal gyrus, planum temporale, and HG.

Correlations of BOLD Signal and the Vividness of Visual Imagery

We used the widely applied VVIQ questionnaire (Marks, 1973) to assess the subjective vividness of visual imagery and predicted that the score might be correlated with the degree of deactivation of the auditory cortex in individual subjects. Figure 7 shows the correlations between the activity levels and the VVIQ scores across subjects. As a first step, we analyzed these correlations in several regions of interest. There is a significant positive correlation between the magnitude of A1 deactivation (negative BOLD signal in auditory cortex) and the subjective vividness of visual imagery (see Figure 7A, left panel, Pearson's $r = 0.67$, $p < 0.05$; Spearman $r = 0.73$, $p < 0.05$). In addition, the positive activation in visual areas shows a trend for positive correlation with the vividness of visual imagery (see Figure 7A, right panel, depicting V1 ROI: Pearson's $r = 0.41$, Spearman $r = 0.32$; $p > 0.05$; a similar pattern is found in the LOC ROI). Note that not all regions showing deactivation to VI show correlations to the VVIQ. For instance, the correlation between VVIQ and negative BOLD is almost flat in the "default-brain network" region PC (Figure 7A, middle panel, $r = 0.01$; $p > 0.9$).

In order to look for possible correlations across the entire brain, we also ran a correlation analysis between VVIQ and BOLD on a voxel-by-voxel exploratory basis. The results of this analysis are presented in Figure 7B and in Table S1 (see the Supplemental Data available online). All significant negative correlations between VI BOLD and VVIQ are located in auditory or somatosensory cortex, including left HG, STG bilaterally, and right STS. In agreement with prior studies, we find positive correlations between VVIQ and BOLD signal in visual and inferior prefrontal cortex (Ishai and Sagi, 1995; Ishai et al., 2000; Kosslyn et al., 1999; Kreiman et al., 2000; Lambert et al., 2004; Mechelli et al., 2004; O'Craven and

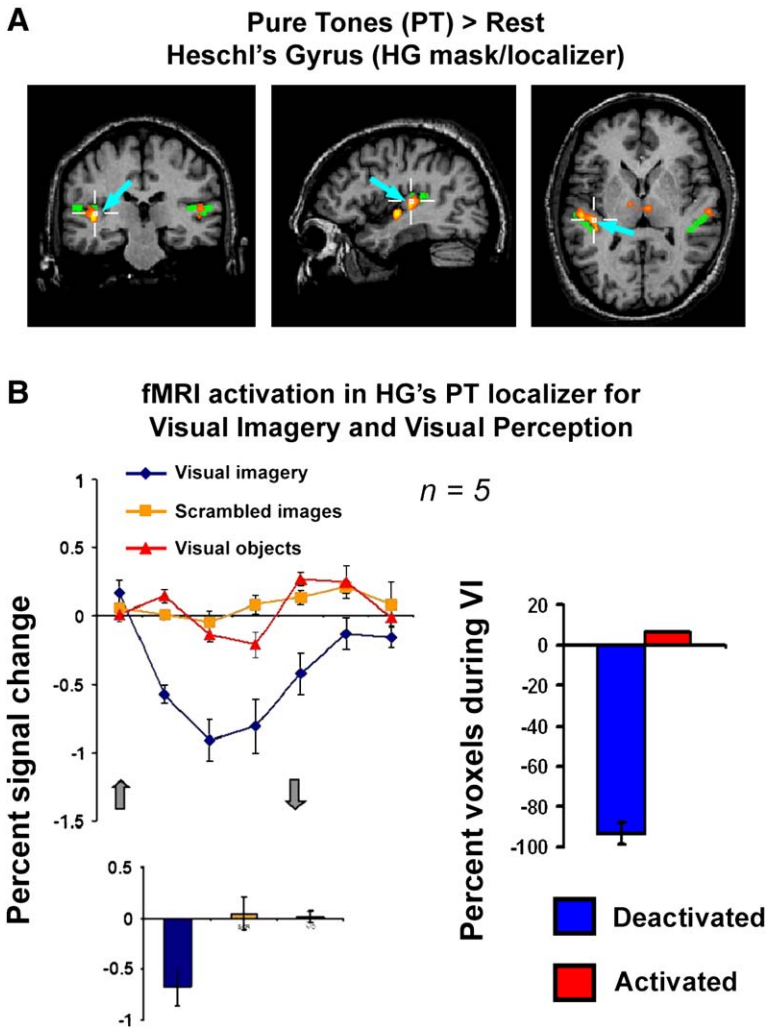

Figure 5. Average Time Course and Average Percent Signal in the Primary Auditory Cortex as Defined by External Pure Tones Localizer

We defined a pure tones region of interest (PT ROI) in order to define an early auditory ROI based on the functional response properties. For this analysis we sampled voxels located in Heschl's gyrus ([A]; cyan arrow) that showed significant responses to pure tones (A). The pattern of response shows similar deactivation for visual imagery, with a typical hemodynamic response (VI, blue diamonds) and no significant response to visual perception of objects (VO, red triangles) or to viewing scrambled versions of the objects (SCR, orange squares; average percent signal changes across subjects ± SEM). We also analyzed the proportion of voxels within this external localizer in each subject showing deactivation versus activation to visual imagery. The vast majority of voxels showed deactivation to VI ([B]; average percent signal changes across subjects ± SEM).

Kanwisher, 2000), but also in parahippocampal areas bilaterally and left parieto-occipital sulcus (Sathian and Zangaladze, 2001).

Inter-Regional Correlations

Thus far, we have shown that auditory and visual cortex show reversed patterns of activation specific to visual imagery. While auditory cortex shows robust deactivation to VI and significant negative correlation to VVIQ, the pattern is reversed in visual cortex. We next tested whether the activation measured during VI in visual cortex should negatively covary with that of auditory cortex both within- and across-subjects (what frequently is referred to in the field as assessing "functional connectivity").

For the within-subject analysis, we used seed activation in left or right LOC. We then performed linear correlations across the entire brain on a voxel-by-voxel basis by using the time courses in the VI and the VO conditions independently (Figure S1). When assessing functional connectivity with the VI response across the brain, there is a robust negative correlation with auditory cortex and parts of somatosensory cortex, and a positive correlation within the contralateral LOC and in PF cortex. When assessing against the VO time course, there are correlations mainly in extrastriate areas of both ventral and dorsal streams, but practically no negative correlations in auditory cortex. While there is some variation between subjects, the results are generally highly consistent across subjects for both conditions. These results support the notion that visual and auditory cortices might have different functional connectivity for visual imagery and visual perception, but in order to show that there are indeed changes in the direct effective connectivity between visual and auditory areas more work needs to be done (see Discussion; for more details see the Supplemental Data).

We also performed an across-subjects analysis of inter-regional covariation on a voxel-by-voxel basis for the VI task data (Horwitz, 1994; Weeks et al., 2000) with the use of the Talairach-transformed brains of each of the nine subjects. The assumption behind this analysis is that if the same network is activated during a given task across subjects and there is variation across subjects in the level of activity, then areas that are part of the network corresponding to a given task should show positive inter-regional covariation. Areas that show positive covariation to the activity in LOC during VI include LOC bilaterally, other ventral retinotopic regions, prefrontal cortex, and posterior parietal cortex (Figure 8,

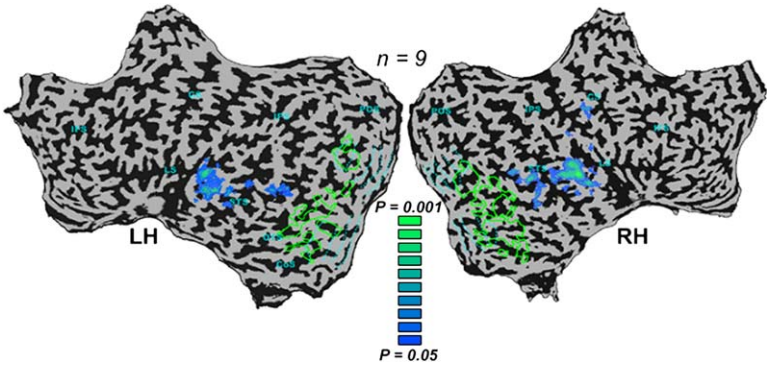

Figure 6. Deactivation of Auditory Cortex during Visual Imagery Is Significantly Stronger than for Visual Objects

To test directly the apparent difference in auditory cortex between visual perception and visual imagery of objects, we used conjunction analysis for visual imagery versus visual objects with deactivation by visual imagery (visual imagery versus rest, negative GLM parameter estimator only). Voxels that show significantly lower activation to VI versus VO and have a negative GLM parameter for VI will appear in a corresponding blue-to-green color scale. The vast majority of these voxels are located in the auditory cortex bilaterally in both early and associative auditory cortex. In addition, some significant clusters are located in the right post-central gyrus and the thalamus (not shown; see Figure 3). When lowering the threshold to $p < 0.0001$ uncorrected, we also find a cluster in the left post-central gyrus. These results confirm the significant difference between the deactivation pattern to visual imagery versus visual perception in auditory cortex and to a lesser extent in somatosensory and subcortical visual areas. (Note: Similar results are evident when contrasting VI and SCR.)

top panel). The highest negative correlations are in auditory cortex, revealing that positive VI activation in visual cortex predicts negative VI activation in auditory cortex across subjects. Some negative correlation is found also in left somatosensory and in medial prefrontal cortex.

To test further this result, we conducted a similar analysis but now choosing the peak voxel in early auditory cortex (HG) as seed. There are positive correlations with the rest of bilateral auditory cortices and bilateral prefrontal and somatosensory cortices, but negative correlations with visual cortex (Figure 8, lower panel).

Discussion

Consistent with previous reports, our results suggest that most brain areas that are activated during visual imagery are also activated by the visual perception of objects (Ishai and Sagi, 1995; Ishai et al., 2000; Kosslyn et al., 1999; Kreiman et al., 2000; Lambert et al., 2004; Mechelli et al., 2004; O'Craven and Kanwisher, 2000). However, the two conditions are dramatically different in their brain-deactivation profile as measured by negative BOLD. In early auditory areas, while there is a minimal response to perception of visual objects, we find robust deactivation during visual imagery. This is demonstrated at group and individual levels of analysis: (1) at the group level by a random-effects GLM analysis of VI versus rest (Figures 1 and 3) or versus visual perception (Figure 6); (2) at the individual subjects level by the high level of consistency in the presence of these VI deactivations bilaterally in all individual subjects studied (Figure 4) and in the pattern of the negative time course, which follows a typical hemodynamic response in associative and early auditory cortex as defined using both anatomical and functional localizers (Figures 2 and 5, respectively). A similar, though less robust, pattern of selective deactivation is also found in somatosensory cortex (post-central gyrus corresponding to S1; Figures 2–4 and 6; Figure 8B) and subcortical structures of the visual pathway (LGN and SC; Figure 3).

Therefore, our main finding is that visual imagery is associated with deactivation of nonvisual sensory processing (auditory cortex and somatosensory cortex) as well as with bottom-up input into early visual areas (LGN and SC). This might functionally isolate the visual cortical system from multisensory and bottom-up influences and thus increase one's ability to create a vivid mental visual image.

The correlation between the level of deactivation and the vividness of visual imagery (Figure 7) further supports the hypothesis that subjects who are able to shut down or disconnect the "irrelevant" cortices are able to imagine visual objects more vividly. However, it is important to note that the VVIQ questionnaire is subjective, and thus this conclusion should be considered with some caution.

Finally, the functional connectivity and inter-regional covariation analysis across subjects (Figure S1 and Figure 8, respectively) further supports the notion of interrelated, reversed patterns of activity in visual and auditory areas during visual imagery. This hypothesis could be further investigated by using advanced effective connectivity methods (Friston, 2002; Friston et al., 1997; Goebel et al., 2003; Horwitz, 1994, 2003).

Crossmodal Deactivation for Visual Imagery and Visual Perception

Some early PET studies demonstrated a decrease in blood flow within auditory cortex during visual perception relative to different baseline conditions (Haxby et al., 1994; Kawashima et al., 1993; Mazziotta et al., 1982). Deactivation of nonvisual areas during visual perception has been demonstrated more recently using fMRI. Laurienti and colleagues (Laurienti et al., 2002) critically assessed the issue of crossmodal interactions and demonstrated crossmodal deactivation of the auditory cortex for viewing alternating checkerboard stimuli (percent signal change ± SD = −0.2 ± 0.3). This effect is comparable in magnitude to what we encountered for our visual SCR condition (−0.15 ± 0.11), which resembles the stimuli used by Laurienti et al. the most. In another fMRI study of visual and auditory motion, Lewis et al. reported deactivation in visual area MT for auditory motion, but did not show the reverse pattern in auditory cortex for visual motion (Lewis et al., 2000). The magnitude of these crossmodal effects during visual perception may truly be significantly smaller when measured with fMRI than with PET. However, this might not always

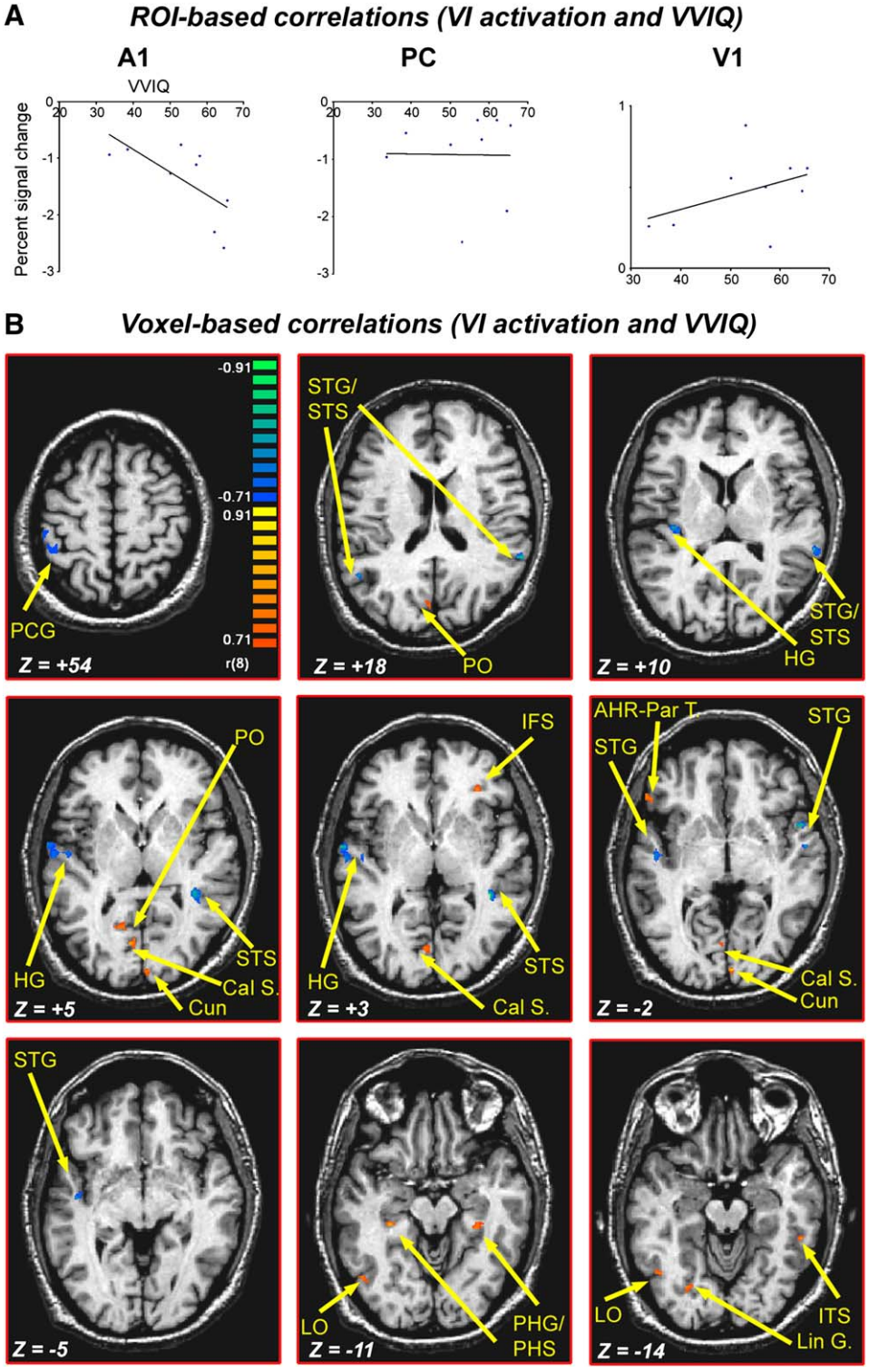

Figure 7. Correlation between VVIQ Scores and VI BOLD Signal

(A) Correlations between the percent signal change for VI in each subject and the VVIQ scores of these individual subjects in three ROIs. We find significant negative correlation between A1 activity and the vividness of the imagery, a trend for positive correlations with V1, and no correlation with PC. (B) Voxel-by-voxel correlations between VI activity and individual VVIQ correlations. Results presented on axial slices covering mainly auditory cortex (for the full set of whole-brain correlation results see Table S1). We find negative correlations in auditory and somatosensory cortex only. Positive correlations were found in visual, prefrontal, and parahippocampal areas bilaterally.

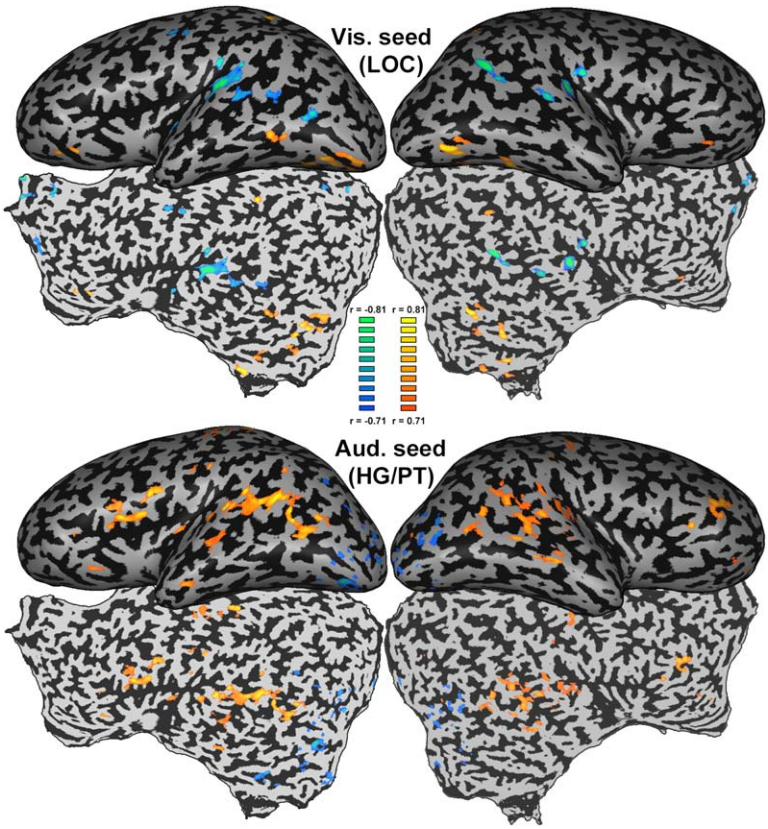

Figure 8. Across-Subjects Covariation of Response between VI Signal in Seed Visual and Auditory Areas and the Rest of the Brain

(A) Using LOC as a seed area. (B) Using A1 as a seed. Correlation coefficient of positive and negative correlations (here the blue-green and red-to-orange color scales depict positive and negative correlation coefficients) on a voxel-by-voxel basis are presented. In both cases, auditory and visual areas show negative covariation in activation during VI while showing different pattern of positive covariation. (Note: Choosing the contralateral LOC or A1 as seed areas reveals generally similar results of negative correlations of visual and auditory cortices.)

be the case; for instance, with the use of PET imaging, recent studies showed significant positive rather than negative BOLD for tactile movement in visual area MT (Hagen et al., 2002) and in other occipital areas during auditory depth perception with the use of an auditory sensory-substitution device (Renier et al., 2005). One hypothesis for the crossmodal deactivation pattern proposes a blood-stealing effect (i.e., as more blood is shunted to visual areas, there is less blood flow available to auditory areas). An alternative explanation for the deactivations suggests a neural link implying a decrease in neuronal firing of the relevant auditory areas and reduced processing and attention to visual input (and vice versa). Perhaps the combination of both of these effects may account for the differences in magnitude between neuroimaging methods. In addition, it is important to note that at the time of some of these earlier studies, random-effects analysis methods were not developed or widely used. This may have led to an overestimation of the magnitude of deactivation during perception.

Given the focus of our study, it is particularly critical to note that none of these studies included a corresponding visual imagery control condition, nor did they contrast the deactivation level during perception and imagery of similar stimuli. Therefore, our results do not contradict prior findings, but expand upon them in two ways. (1) We show that the observed deactivation during visual perception of noise patterns is also demonstrable during imagery. (2) More importantly, we show that the magnitude of the deactivation is significantly greater during imagery than during perception of both objects and noise patterns (Figures 1, 2, 5, and 6). Interestingly, the blood-stealing model predicts that visual imagery should result in *less* deactivation, as the magnitude and extent of positive BOLD activation in visual areas (and across the entire brain) is much more modest than during visual perception (see Figures 1 and 2). Finding the reverse pattern supports the notion that the noted deactivation is not a result of a blood-stealing effect, but in fact is related to changes in the firing patterns and synaptic activity of neurons (Laurienti, 2004; Shmuel et al., 2002; Wade, 2002; A. Shmuel et al., 2003, NeuroImage, abstract).

During visual perception, multiple sensory modalities interact and shape the resulting visual experience. For example, auditory or tactile stimuli can influence the perceived duration, rate, or intensity of a visual stimulus or even the interpretation of a visual event as moving, bouncing, or stationary (Shimojo and Shams, 2001). In fact, seeing in the absence of sound can activate the primary auditory cortex (Calvert et al., 1997) and vice versa (for review see Pascual-Leone et al., 2005). Similarly, auditory or tactile stimulation can modulate activity in the visual cortex (Macaluso et al., 2000; Shams et al., 2001). In contrast, visual imagery occurs when the visual scene is no longer being viewed and a visual short-term memory representation of it is evoked. We hypothesize that in this context the lack of crossmodal interactions might in fact be critical to creating the experiential distinction between visual perception and visual imagery. Thus, vivid visual imagery requires the activation of visual areas but also the deactivation of nonvisual cortical regions.

Possible Confounding Factors Contributing to the Reported Deactivation Pattern

Scanner Noise

We have demonstrated that deactivation of auditory cortex (and other nonvisual areas) is an important feature of the neural correlates of visual imagery. A remaining question is why this deactivation is so prominent in auditory cortex in comparison to other nonvisual cortical regions (Figures 1 and 3). It might be speculated that the noisy environment of the MRI scanner increases the need to shut down auditory cortex activity in order to enable successful visual imagery. For instance, it might be speculated that visual perception induces large deactivations in A1, which are counterbalanced by auditory stimulation from gradient noise, and that this is why we might see only a modest deactivation in A1 for real stimuli in fMRI. However, the same gradient noise is also present during the rest and the visual imagery conditions and thus cannot solely explain the present results. Crossmodal inhibition during a difficult, attention-demanding task (Laurienti et al., 2002) may contribute to, but cannot fully account for, our results. Furthermore, the noisy MRI environment does not seem to be a necessary requirement for the deactivation of auditory cortex during imagery. Halpern and colleagues (Halpern et al., 2004) found that the secondary auditory cortex shows positive BOLD during perception and imagery of auditory timbre with the use of a fMRI sparse-sampling approach that allowed them to perform the tasks in quiet intervals between data acquisition periods. In agreement with our results, this region shows deactivation during a control visual imagery task in relation to a rest period, although the imagery task was performed during the quiet interval. Thus, auditory cortex deactivation for visual imagery appears to occur also in less noisy settings. Unfortunately, the aforementioned study was not designed to contrast visual imagery with visual perception directly, but our results seem to confirm and expand upon these findings.

Eyes Open, Eyes Closed

In the present study, subjects had their eyes closed during imagery, but open during visual perception. This introduces a possible confounding factor, as it was shown recently that closed eyes can induce in certain circumstances deactivation in visual, auditory, and somatosensory cortex, as well as other areas (Marx et al., 2004). However, it is important to note that in our case the rest period before each imagery condition was with the eyes closed (to serve as a relevant baseline to the following imagery condition). Thus, the deactivation presented in Figure 2 could not result from this difference alone (i.e., the first two time points reflect what happened in the rest period with eyes closed). The agreement between our results and those of Halpern and colleagues (Halpern et al., 2004) also argues against a critical impact of eyes open versus closed, as they found deactivation of auditory cortex during visual imagery even though their subjects performed the task with eyes open. Finally, we have added data from an additional experiment to further address this issue, which is presented in Figure S2.

"Default Brain" Network and Visual Imagery

Most previous reports on deactivation patterns have focused on a network of posterior-medial parietal (PC), medial prefrontal, and lateral parieto-temporal areas originally termed the "default brain" network (Raichle et al., 2001). The working hypothesis was that deactivation of these areas during a goal-directed cognitive task reflects the interruption of internal processes going on during rest (e.g., "stream of thoughts"). We show here that visual imagery deactivates this network (at least in PC) as much as visual perception of objects and thus may be considered in the context of the default brain hypothesis as a goal-directed task. This result is consistent with the notion that visual imagery represents an active cognitive process and that to some extent the brain "treats" the created mental images as real physical stimuli.

Conclusions and General Framework

Perception of the world requires the merging of multisensory information, and seeing is inextricably associated with the processing of other sensory modalities that modify visual cortical activity and shape experience (for reviews see Amedi et al., 2005; Beauchamp, 2005; Driver and Spence, 1998; Pascual-Leone et al., 2005; Pascual-Leone and Hamilton, 2001; Stein and Meredith, 1993). In contrast, we suggest here that pure visual imagery is characterized by an isolated activation of visual cortical areas with concurrent deactivation of sensory inputs that could potentially disrupt the image created by our mind's eye. This is likely to be in sharp contrast to multisensory mental imagery, e.g., musicians who often visualize themselves playing their instrument, evoking the sensation and mentally rehearsing the sequence of finger movements involved, while listening in their mind's ear to the music (e.g., Pascual-Leone, 2001).

An alterative hypothesis to account for our results is that deactivation is the consequence of filtering out irrelevant stimuli. Perceiving real objects does not require much filtering because they are so salient; however, the signal-to-noise ratio is much smaller during mental imagery and thus may require more filtering to obtain image saliency. Note that this hypothesis is not mutually exclusive to our original interpretation—i.e., imagery is a special case of such filtering out of irrelevant information in situations of a "problematic" signal-to-noise ratio. There are some predictions of this alternative model that will need to be tested in the future. For instance, adding tactile noise (e.g., massive brushing on body) during the whole experiment might increase negative BOLD in S1 during visual imagery.

Finally, the mechanism that creates this robust deactivation is still unclear. It might simply reflect less neuronal activity in auditory cortex (and other "irrelevant" sensory areas) during visual imagery in comparison to visual perception or even rest. Alternatively, this deactivation might be the result of an active suppression process that is triggered by a separate brain region. For instance, it was shown recently that the PF cortex contributes to the top-down initiation of visual imagery in visual areas (Ishai et al., 2000, 2002; Mechelli et al., 2004). The reported pattern of correlations between PF, A1, and LOC might support this top-down role of PF cortex in imagery also for the negative BOLD effect, but this too needs to be further investigated in order to establish a causal rather than correlational relationship. Thus far, we have only demonstrated functional rather than

effective connectivity (Figure 8 and Figure S1), as two neural entities are said to be "functionally connected" if their activities are correlated. More sophisticated effective connectivity techniques refer to the direct influence of one neural entity on a second one and are necessary to truly explore causal relationships with the use of neuroimaging techniques (Friston, 2002; Friston et al., 1997; Goebel et al., 2003; Horwitz, 1994, 2003; Mechelli et al., 2004). Alternatively, similar issues can be addressed with the use of transcranial magnetic stimulation to create virtual lesions (Pascual-Leone et al. 2000) or with combined fMRI-TMS techniques (Bohning et al., 1998; Baudewig et al., 2000; Bestmann et al., 2003; A. Amedi et al., 2005, Soc. Neurosci., abstract).

Experimental Procedures

MRI Acquisition

The BOLD fMRI measurements were performed in a whole-body 1.5 T, Signa Horizon, LX8.25 General Electric scanner. The MRI system was equipped with 22 mT/m field gradients with a slew rate of 120 T/m/s (Echospeed). 3D anatomical volumes were collected using a T1 SPGR sequence. The functional MRI protocols were based on a multislice gradient echo, echo-planar imaging (EPI), and a standard head coil. The functional data were obtained under the optimal timing parameters: TR = 3 s, TE = 55 ms, flip angle = 90°, imaging matrix = 80 × 80, FOV = 24 cm. The 17 slices with slice thickness 4 mm and 1 mm gap were oriented approximately in the axial position, covering the whole brain except the most dorsal and ventral tips.

Experimental Setup

The stimulus sequences were generated on a PC and projected via an LCD projector (Epson MP 7200) onto a tangent screen located inside the scanner and in front of the subject.

Subjects

Nine volunteers without neurological or psychiatric problems (4 women and 5 men, ages 27–50 years) participated in the study. Six were right handed and three left handed as assessed by the Oldfield Handedness Questionnaire. The institutional review board approved the experimental procedure. A written informed consent was obtained from each subject.

Stimuli and Experimental Design

The experiment included three different experimental conditions in a block-design paradigm: a visual objects recognition task (VO) and viewing scrambled images of the same objects (SCR) while fixating using a standardized set of visual objects presented at a 1 Hz rate, and a visual imagery condition (VI). In VI, subjects were orally instructed in each block to visually imagine with their eyes closed three objects (they had seen these objects extensively before the scan). Pilot testing showed that it takes a few seconds to really be able to imagine the object's image. We used several objects because we preferred to work in a block design where the signal is building up. This might be especially important in imagery, which in many studies tends to show lower signals in comparison to perception (e.g., Ishai et al., 2000; Kosslyn et al., 1999; Mechelli et al., 2004; O'Craven and Kanwisher, 2000). The subject determined the transitions between objects, while asking to maintain the last object until the stop cue. The short verbal instructions (to see or imagine in the beginning of the epochs and stop in the end) were shared by all three experimental conditions.

Data Analysis

Data analysis was performed using Brain Voyager 4.96 and Brain Voyager QX 1.4 software package (Brain Innovation, Maastricht, The Netherlands). This included preprocessing stages and general linear analysis (GLM). Preprocessing included head motion correction, slice scan time correction, and high-pass temporal smoothing in the frequency domain to remove drifts and to improve signal-to-noise ratio. To compute statistical parametric maps we applied a GLM with the use of predictors convoluted with a typical hemodynamic response function (using parameters as in Boynton et al., 1996). Across-subject statistical parametric maps were calculated by using hierarchical random-effects model analysis (Friston et al., 1999) after transformation into Talairach space (Talairach, 1988). Significance levels were calculated taking into account the probability of a false detection for any given cluster (Forman et al., 1995). The minimum significance level, corrected for any given cluster was $p < 0.05$.

Single-Subject 3D Recording and Cortex Reconstruction

Separate 3D recordings were used for surface reconstruction of all nine subjects. This procedure included the segmentation of the white matter by using a grow-region function. The cortical surface was then inflated and unfolded, cut along the calcarine sulcus, and flattened. The obtained activation maps were superimposed on the inflated and unfolded cortex for each subject. The Talairach coordinates were determined for each region of interest.

Time Course and Percent Signal Change Analysis

Activation was sampled from various ROIs for visual imagery versus rest separately in each individual (using the peak voxel in a smoothed volume, after convolution with a Gaussian kernel of 4 mm full-width at half-maximum) and regardless of whether the voxel was peak maximum or minimum. Then the averaged percent signal change and the standard errors were calculated for each condition. The magnitude of activation was sampled from eight regions of interest (Figure 2). (1) Primary auditory cortex (A1 ROI), which was defined either anatomically (Heschl's gyrus; Figure 2) or functionally by using a pure tones localizer (Figure 5). For more details on the relation between primary auditory cortex, its newly discovered subdivisions, and its relation to anatomical markers see Morosan et al. (2001), Penhune et al. (1996), Rademacher et al. (2001), and below. (2) Superior temporal sulcus (STS ROI) in the auditory cortex, based on anatomical marker. (3) V1 (calcarine sulcus), based on retinotopic mapping (see below). (4) LOC, the visual object-related lateral-occipital complex was defined by a functional localizer contrasting VO and SCR (Grill-Spector and Malach, 2004). (5) Ventral prefrontal cortex (PF ROI, the peak voxel ventral to superior frontal gyrus and anterior to the central sulcus; activation was typically located in pars opercularis or a bit more anterior to it). (6) Post-central gyrus (PCG ROI), identified anatomically by using single-subject inflated surface reconstruction. (7) Posterior cingulate (PC) "default brain" area. (8) PO ROI. This is another occipital ROI, in which we picked up the peak voxel in the occipital lobe, which was most adjacent to parieto-occipital sulcus, (i.e., posterior to posterior-occipital sulcus: PO ROI). The rationale for this ROI was our observation (see statistical parametric maps) that the parieto-occipital sulcus seems to separate nicely regions of positive and negative BOLD to both visual perception and visual imagery, and we wanted to test the time course and percent signal change profiles in these two ROIs (PC and PO).

Retinotopic Mapping

The borders of retinotopic visual areas were determined based on mapping the vertical and horizontal visual field meridians for each subject (DeYoe et al., 1996; Engel et al., 1997; Sereno et al., 1995). This map was obtained in a separate scan in which the subjects viewed triangular wedges either containing natural grayscale images or flickering black and white random dots. The flickering dots were effective in mapping borders between areas V1 and V2, and the natural grayscale images were useful for distinguishing higher-order areas (Levy et al., 2001).

"Pure Tones" Localizer

We defined a pure tones region of interest (PT ROI) in order to use an alternative way to define early auditory ROIs based on the auditory functional response properties in Heschl's gyrus and not only based on anatomy. We used a block-design paradigm with two main conditions: "pure tones" and rest. The pure tones blocks contained 24 tones presented at 2 Hz. The duration of each tone was 350 ms, with linear onset and offset ramps of 5 ms. Three block types were created, each containing tones in a different frequency range: low (200–300 Hz), medium (800–1200 Hz), and high (3200–4800 Hz). Each block type was repeated six times to make a total of 18 blocks.

The frequency of the tones in the low blocks (6 × 24 = 144 tones) was chosen from a uniform distribution over the frequency interval 200–300 Hz. For each of the six low-tone blocks thus created, corresponding medium and high blocks were created that contain the same melodic sequences, shifted by two octaves or four octaves up. As pure tones were only used to define early auditory cortex in general and not to assess tonotopic maps, we combined all these blocks into one predictor (PT). Specifically, we used here a combination of functional and anatomical markers. We took all the voxels located in Heschl's gyrus that were significantly activated by pure tones (Figure 5A shows this procedure in one representative subject). This was intended to give us a functional signature of early auditory areas. We then used this mask to sample the individual time course and percent signal change from each subject. The averages and SEM are presented in Figure 5B. Finally, we present the proportions of individual voxels showing activation or deactivation to VI. This was done by sorting the individual estimate parameter of the VI predictor (the β values of the GLM model) in these ROIs in each subject to positive and negative, computing the proportion of each and averaging across subjects (Figure 5B). This localizer scan and procedure was run in five of the nine subjects that participated in the experiments.

Subjective Visual Imagery Score and Its Correlation to the BOLD Signal

Following the fMRI scanning, the Vividness of Visual Imagery Questionnaire (VVIQ; Marks, 1973; Zhang et al., 2004) was completed by each subject. This questionnaire contains a series of questions testing the vividness of imagined scenes or objects on a five-rating scale. Following the advice of expert users of this questionnaire, we flipped the scale (so that 5 represented maximum imagery, and 1 minimum imagery, as this tends to be a more natural way to report the vividness of created visual mental image). Thus, the higher the VVIQ score, the more vivid the visual imagery that the subject reported (the full version of the questionnaire is included in the Supplemental Data). We assessed three scores: with eyes closed, with eyes open, and an average of the two (the average results in our group were 55.9 ± 4.0 SEM; 51.2 ± 4.1, and 53.6 ± 4.0, respectively). The results of the correlations presented in Figure 7 and Table S1 represent the third score. In actuality, the correlation with eyes closed was higher and more significant in A1 (and most other ROIs), but we chose the more conservative average score. This score was correlated with the BOLD signal intensity of the peak voxel in a smoothed volume within each ROI, after convolution with a Gaussian kernel of 4 mm full-width at half-maximum (FWHM). Significance was computed both with Pearson (parametric correlations) and Spearman (nonparametric correlations) tests (Figure 7A) or on a voxel-by-voxel exploratory basis (Figure 7B). In the voxel-by-voxel correlations, the data of each subject were transformed to Talairach space and smoothed spatially with Gaussian kernel of 4 mm FWHM. For each voxel, the parameter estimator of the VI condition was computed using a standard GLM analysis. This resulted in a set of nine VI parameter estimates for each voxel in Talairach space, which was in then correlated to the VVIQ score.

Within-Subject Functional Connectivity

See Supplemental Data for details.

Across-Subjects Within-Task Inter-Regional Correlations

We looked for significant inter-regional correlations across the subjects on a voxel-by-voxel basis. To assess such functional connectivity across subjects, we used a technique adapted from Horwitz and colleagues (Horwitz, 1994; Weeks et al., 2000). In the first step, we performed spatial smoothing of individual subjects' data by using a Gaussian kernel of 4 mm FWHM to enhance spatial coregistration and to average each voxel with its closest neighbors in a Gaussian manner. Next, all brains were transformed into Talairach space (Talairach, 1988). We then assessed the activation level for the VI condition in all nine subjects independently in two seed areas (LOC and HG; in both cases using the peak deactivation in auditory cortex located in HG and the peak activation in LOC in the multisubject random-effect analysis GLM). Next, we searched for interregional covariation across subjects from these seed areas across the entire brain. This resulted in statistical parametric maps in which the color-coded index represents linear correlation values between the seed and all other voxels. The threshold of the correlations level was set to $r(8) = \pm 0.71$, $p < 0.05$.

Supplemental Data

The Supplemental Data for this article can be found online at http://www.neuron.org/cgi/content/full/48/5/859/DC1/.

Acknowledgments

The work on this article was supported by grants from the National Institutes of Health (K24 RR018875 and RO1-EY12091 to A.P.-L.), the Human Frontiers Science Program foundation award (to A.A). The authors would like to thank M. Thivierge for constant administrative support; E. Zohary and L.B. Merabet for their invaluable input; and N. Bass-Pitskel for English editing; M. Harel for help with cortex reconstruction; and G. Jacobson for help with auditory localizer.

Received: June 27, 2005
Revised: September 20, 2005
Accepted: October 27, 2005
Published: December 7, 2005

References

Amedi, A., Malach, R., Hendler, T., Peled, S., and Zohary, E. (2001). Visuo-haptic object-related activation in the ventral visual pathway. Nat. Neurosci. *4*, 324–330.

Amedi, A., Von Kriegstein, K., Van Atteveldt, N., Beauchamp, M.S., and Naumer, M.J. (2005). Functional imaging of human crossmodal identification and object recognition. Exp. Brain Res. *166*, 559–571.

Baudewig, J., Paulus, W., and Frahm, J. (2000). Artifacts caused by transcranial magnetic stimulation coils and EEG electrodes in T(2)*-weighted echo-planar imaging. Magn. Reson. Imaging *18*, 479–484.

Beauchamp, M.S. (2005). See me, hear me, touch me: multisensory integration in lateral occipital-temporal cortex. Curr. Opin. Neurobiol. *15*, 145–153.

Beauchamp, M.S., Lee, K.E., Argall, B.D., and Martin, A. (2004). Integration of auditory and visual information about objects in superior temporal sulcus. Neuron *41*, 809–823.

Bestmann, S., Baudewig, J., and Frahm, J. (2003). On the synchronization of transcranial magnetic stimulation and functional echo-planar imaging. J. Magn. Reson. Imaging *17*, 309–316.

Bohning, D.E., Shastri, A., Nahas, Z., Lorberbaum, J.P., Andersen, S.W., Dannels, W.R., Haxthausen, E.U., Vincent, D.J., and George, M.S. (1998). Echoplanar BOLD fMRI of brain activation induced by concurrent transcranial magnetic stimulation. Invest. Radiol. *33*, 336–340.

Boynton, G.M., Engel, S.A., Glover, G.H., and Heeger, D.J. (1996). Linear systems analysis of functional magnetic resonance imaging in human V1. J. Neurosci. *16*, 4207–4221.

Calvert, G.A., Bullmore, E.T., Brammer, M.J., Campbell, R., Williams, S.C., McGuire, P.K., Woodruff, O.W., Iversen, S.D., and David, A.S. (1997). Activation of auditory cortex during silent lipreading. Science *276*, 593–596.

DeYoe, E.A., Carman, G.J., Bandettini, P., Glickman, S., Wieser, J., Cox, R., Miller, D., and Neitz, J. (1996). Mapping striate and extrastriate visual areas in human cerebral cortex. Proc. Natl. Acad. Sci. USA *93*, 2382–2386.

Driver, J., and Spence, C. (1998). Crossmodal attention. Curr. Opin. Neurobiol. *8*, 245–253.

Engel, S.A., Glover, G.H., and Wandell, B.A. (1997). Retinotopic organization in human visual cortex and the spatial precision of functional MRI. Cereb. Cortex *7*, 181–192.

Forman, S.D., Cohen, J.D., Fitzgerald, M., Eddy, W.F., Mintun, M.A., and Noll, D.C. (1995). Improved assessment of significant activation in functional magnetic resonance imaging (fMRI): use of a cluster-size threshold. Magn. Reson. Med. *33*, 636–647.

Friston, K. (2002). Beyond phrenology: what can neuroimaging tell us about distributed circuitry? Annu. Rev. Neurosci. *25*, 221–250.

Friston, K.J., Buechel, C., Fink, G.R., Morris, J., Rolls, E., and Dolan, R.J. (1997). Psychophysiological and modulatory interactions in neuroimaging. Neuroimage *6*, 218–229.

Friston, K.J., Holmes, A.P., and Worsley, K.J. (1999). How many subjects constitute a study? Neuroimage *10*, 1–5.

Goebel, R., Roebroeck, A., Kim, D.S., and Formisano, E. (2003). Investigating directed cortical interactions in time-resolved fMRI data using vector autoregressive modeling and Granger causality mapping. Magn. Reson. Imaging *21*, 1251–1261.

Greicius, M.D., and Menon, V. (2004). Default-Mode Activity during a Passive Sensory Task: Uncoupled from Deactivation but Impacting Activation. J. Cogn. Neurosci. *16*, 1484–1492.

Grill-Spector, K., and Malach, R. (2004). The human visual cortex. Annu. Rev. Neurosci. *27*, 649–677.

Gusnard, D.A., and Raichle, M.E. (2001). Searching for a baseline: functional imaging and the resting human brain. Nat. Rev. Neurosci. *2*, 685–694.

Hagen, M.C., Franzen, O., McGlone, F., Essick, G., Dancer, C., and Pardo, J.V. (2002). Tactile motion activates the human middle temporal/V5 (MT/V5) complex. Eur. J. Neurosci. *16*, 957–964.

Halpern, A.R., Zatorre, R.J., Bouffard, M., and Johnson, J.A. (2004). Behavioral and neural correlates of perceived and imagined musical timbre. Neuropsychologia *42*, 1281–1292.

Haxby, J.V., Horwitz, B., Ungerleider, L.G., Maisog, J.M., Pietrini, P., and Grady, C.L. (1994). The functional organization of human extrastriate cortex: a PET-rCBF study of selective attention to faces and locations. J. Neurosci. *14*, 6336–6353.

Horwitz, B. (1994). Data analysis paradigms for metabolic flow data: combining neural modeling and functional imaging. Hum. Brain Mapp. *2*, 112–122.

Horwitz, B. (2003). The elusive concept of brain connectivity. Neuroimage *19*, 466–470.

Ishai, A., and Sagi, D. (1995). Common mechanisms of visual imagery and perception. Science *268*, 1772–1774.

Ishai, A., Ungerleider, L.G., and Haxby, J.V. (2000). Distributed neural systems for the generation of visual images. Neuron *28*, 979–990.

Ishai, A., Haxby, J.V., and Ungerleider, L.G. (2002). Visual imagery of famous faces: effects of memory and attention revealed by fMRI. Neuroimage *17*, 1729–1741.

Kawashima, R., O'Sullivan, B.T., and Roland, P. (1993). A PET study of selective attention in man: cross-modality decreases in activity in somatosensory and visual tasks. J. Cereb. Blood Flow Metab. *13*, S502.

Klein, I., Dubois, J., Mangin, J.F., Kherif, F., Flandin, G., Poline, J.B., Denis, M., Kosslyn, S.M., and Le Bihan, D. (2004). Retinotopic organization of visual mental images as revealed by functional magnetic resonance imaging. Brain Res. Cogn. Brain Res. *22*, 26–31.

Kosslyn, S.M., Pascual-Leone, A., Felician, O., Camposano, S., Keenan, J.P., Thompson, W.L., Ganis, G., Sukel, K.E., and Alpert, N.M. (1999). The role of area 17 in visual imagery: convergent evidence from PET and rTMS. Science *284*, 167–170.

Kreiman, G., Koch, C., and Fried, I. (2000). Imagery neurons in the human brain. Nature *408*, 357–361.

Lambert, S., Sampaio, E., Mauss, Y., and Scheiber, C. (2004). Blindness and brain plasticity: contribution of mental imagery? An fMRI study. Brain Res. Cogn. Brain Res. *20*, 1–11.

Laurienti, P.J. (2004). Deactivations, global signal, and the default mode of brain function. J. Cogn. Neurosci. *16*, 1481–1483.

Laurienti, P.J., Burdette, J.H., Wallace, M.T., Yen, Y.F., Field, A.S., and Stein, B.E. (2002). Deactivation of sensory-specific cortex by cross-modal stimuli. J. Cogn. Neurosci. *14*, 420–429.

Levy, I., Hasson, U., Avidan, G., Hendler, T., and Malach, R. (2001). Center-periphery organization of human object areas. Nat. Neurosci. *4*, 533–539.

Lewis, J.W., Beauchamp, M.S., and DeYoe, E.A. (2000). A comparison of visual and auditory motion processing in human cerebral cortex. Cereb. Cortex *10*, 873–888.

Logothetis, N.K., and Wandell, B.A. (2004). Interpreting the BOLD signal. Annu. Rev. Physiol. *66*, 735–769.

Macaluso, E., Frith, C.D., and Driver, J. (2000). Modulation of human visual cortex by crossmodal spatial attention. Science *289*, 1206–1208.

Marks, D.F. (1973). Visual imagery differences in the recall of pictures. Br. J. Psychol. *64*, 17–24.

Marx, E., Deutschlander, A., Stephan, T., Dieterich, M., Wiesmann, M., and Brandt, T. (2004). Eyes open and eyes closed as rest conditions: impact on brain activation patterns. Neuroimage *21*, 1818–1824.

Mazziotta, J.C., Phelps, M.E., Carson, R.E., and Kuhl, D.E. (1982). Tomographic mapping of human cerebral metabolism: auditory stimulation. Neurology *32*, 921–937.

Mechelli, A., Price, C.J., Friston, K.J., and Ishai, A. (2004). Where bottom-up meets top-down: neuronal interactions during perception and imagery. Cereb. Cortex *14*, 1256–1265.

Merabet, L., Thut, G., Murray, B., Andrews, J., Hsiao, S., and Pascual-Leone, A. (2004). Feeling by sight or seeing by touch? Neuron *42*, 173–179.

Morosan, P., Rademacher, J., Schleicher, A., Amunts, K., Schormann, T., and Zilles, K. (2001). Human primary auditory cortex: cytoarchitectonic subdivisions and mapping into a spatial reference system. Neuroimage *13*, 684–701.

O'Craven, K.M., and Kanwisher, N. (2000). Mental imagery of faces and places activates corresponding stimulus-specific brain regions. J. Cogn. Neurosci. *12*, 1013–1023.

Pascual-Leone, A. (2001). The brain that plays music and is changed by it. Ann. NY Acad. Sci. *930*, 315–329.

Pascual-Leone, A., and Hamilton, R. (2001). The metamodal organization of the brain. In Vision: From Neurons to Cognition, C. Casanova, and M. Ptito, eds. (New York: Elsevier), pp. 427–445.

Pascual-Leone, A., Dang, N., Cohen, L.G., Brasil-Neto, J.P., Cammarota, A., and Hallett, M. (1995). Modulation of human cortical motor outputs during the acquisition of new fine motor skills. J. Neurophysiol. *74*, 1037–1045.

Pascual-Leone, A., Walsh, V., and Rothwell, J. (2000). Transcranial magnetic stimulation in cognitive neuroscience - virtual lesion, chronometry, and functional connectivity. Curr. Opin. Neurobiol. *10*, 232–237.

Pascual-Leone, A., Amedi, A., Fregni, F., and Merabet, L.B. (2005). The Plastic Human Brain Cortex. Annu. Rev. Neurosci. *28*, 377–401.

Penhune, V.B., Zatorre, R.J., MacDonald, J.D., and Evans, A.C. (1996). Interhemispheric anatomical differences in human primary auditory cortex: probabilistic mapping and volume measurement from magnetic resonance scans. Cereb. Cortex *6*, 661–672.

Rademacher, J., Morosan, P., Schormann, T., Schleicher, A., Werner, C., Freund, H.J., and Zilles, K. (2001). Probabilistic mapping and volume measurement of human primary auditory cortex. Neuroimage *13*, 669–683.

Raichle, M.E., MacLeod, A.M., Snyder, A.Z., Powers, W.J., Gusnard, D.A., and Shulman, G.L. (2001). A default mode of brain function. Proc. Natl. Acad. Sci. USA *98*, 676–682.

Renier, L., Collignon, O., Poirier, C., Tranduy, D., Vanlierde, A., Bol, A., Veraart, C., and De Volder, A.G. (2005). Cross-modal activation of visual cortex during depth perception using auditory substitution of vision. Neuroimage *26*, 573–580.

Sathian, K., and Zangaladze, A. (2001). Feeling with the mind's eye: the role of visual imagery in tactile perception. Optom. Vis. Sci. *78*, 276–281.

Sereno, M.I., Dale, A.M., Reppas, J.B., Kwong, K.K., Belliveau, J.W., Brady, T.J., Rosen, B.R., and Tootell, R.B. (1995). Borders of multiple visual areas in humans revealed by functional magnetic resonance imaging. Science *26*, 889–893.

Shams, L., Kamitani, Y., Thompson, S., and Shimojo, S. (2001). Sound alters visual evoked potentials in humans. Neuroreport *12*, 3849–3852.

Shimojo, S., and Shams, L. (2001). Sensory modalities are not separate modalities: plasticity and interactions. Curr. Opin. Neurobiol. *11*, 505–509.

Shmuel, A., Yacoub, E., Pfeuffer, J., Van de Moortele, P.F., Adriany, G., Hu, X., and Ugurbil, K. (2002). Sustained negative BOLD, blood flow and oxygen consumption response and its coupling to the positive response in the human brain. Neuron *36*, 1195–1210.

Stein, B.E., and Meredith, M.A. (1993). The Merging of the Senses (Cambridge, MA: The MIT Press).

Talairach, J.T.P. (1988). Co-Planar Stereotaxic Atlas of the Human Brain (New York: Thieme).

Wade, A.R. (2002). The negative BOLD signal unmasked. Neuron *36*, 993–995.

Weeks, R., Horwitz, B., Aziz-Sultan, A., Tian, B., Wessinger, M., Cohen, L.G., Hallett, M., and Rauchecker, J.P. (2000). A positron emission tomography study of auditory localization in the congenitally blind. J. Neurosci. *20*, 2664–2672.

Zhang, M., Weisser, V.D., Stilla, R., Prather, S.C., and Sathian, K. (2004). Multisensory cortical processing of object shape and its relation to mental imagery. Cogn. Affect. Behav. Neurosci. *4*, 251–259.